

# Phase matching in hyperbolic wire media for nonlinear frequency conversion

Yuchen Zhao,<sup>1,2</sup> Cameron Duncan,<sup>1</sup> Boris T. Kuhlmeiy,<sup>1</sup> and C. Martijn de Sterke<sup>1,\*</sup>

<sup>1</sup>Centre for Ultrahigh bandwidth Devices for Optical Systems (CUDOS) and Institute of Photonics and Optical Science (IPOS), School of Physics, University of Sydney, NSW 2006, Australia

<sup>2</sup>Télécom Physique Strasbourg, University of Strasbourg, 67412 Illkirch, France

\*[martijn.desterke@sydney.edu.au](mailto:martijn.desterke@sydney.edu.au)

**Abstract:** Efficient nonlinear frequency conversion requires a phase matching condition to be satisfied. We analyze the dispersion of the modes of hyperbolic wire metamaterials and demonstrate that phase matching at infrared wavelengths can be achieved with a variety of constituent materials, such as GaAs, in which phase matching cannot easily be achieved by conventional means. Our finding promises access to many materials with attractive nonlinear properties.

©2015 Optical Society of America

OCIS codes: (160.3918) Metamaterials; (190.0190) Nonlinear optics.

---

## References and links

1. R. W. Boyd, *Nonlinear Optics*, 2nd ed. (Academic Press, 2003), Ch. 2.
2. P. E. Powers, *Fundamentals of Nonlinear Optics* (CRC Press, 2011), Ch. 5.
3. V. Berger, A. Fiore, E. Rosencher, P. Bravetti, and J. Nagle, "Phase matching using an isotropic nonlinear optical material," *Nature* **391**(6666), 463–466 (1998).
4. M. M. Fejer, G. A. Magel, D. H. Jundt, and R. L. Byer, "Quasi-phase-matched second harmonic generation: tuning and tolerances," *IEEE J. Quantum Electron.* **28**(11), 2631–2654 (1992).
5. M. J. Steel and C. M. de Sterke, "Second-harmonic generation in second-harmonic fiber Bragg gratings," *Appl. Opt.* **35**(18), 3211–3222 (1996).
6. M. Centini, C. Sibilia, M. Scalora, G. D'Aguanno, M. Bertolotti, M. J. Bloemer, C. M. Bowden, and I. Nefedov, "Dispersive properties of finite, one-dimensional photonic band gap structures: applications to nonlinear quadratic interactions," *Phys. Rev. E Stat. Phys. Plasmas Fluids Relat. Interdiscip. Topics* **60**(4 Pt B), 4891–4898 (1999).
7. J. Torres, G. Vecchi, D. Coquillat, M. A. Malvezzi, R. Legros, J. P. Lascaray, D. Peyrade, Y. Chen, M. Le Vassor d'Yerville, E. Centeno, D. Cassagne, J. P. Albert, and R. M. De La Rue, "Enhancement of second harmonic generation in one-dimensional and two-dimensional epitaxial GaN-based photonic crystals," in *Photonic Crystal Materials and Nanostructures*, R. M. DeLaRue, P. Viktorovitch, C. M. S. Torres, and M. Midrio, eds. (SPIE, 2004), pp. 240–249.
8. M. Scalora, M. J. Bloemer, A. S. Manka, J. P. Dowling, C. M. Bowden, R. Viswanathan, and J. W. Haus, "Pulsed second-harmonic generation in nonlinear, one-dimensional, periodic structures," *Phys. Rev. A* **56**(4), 3166–3174 (1997).
9. C. R. Simovski, P. A. Belov, A. V. Atrashchenko, and Y. S. Kivshar, "Wire metamaterials: physics and applications," *Adv. Mater.* **24**(31), 4229–4248 (2012).
10. I. V. Shadrivov, A. A. Zharov, and Yu. S. Kivshar, "Second-harmonic generation in nonlinear left-handed metamaterials," *J. Opt. Soc. Am. B* **23**(3), 529–534 (2006).
11. Z. Kudyshev, I. Gabitov, and A. Maimistov, "Effect of phase mismatch on second-harmonic generation in negative-index materials," *Phys. Rev. A* **87**(6), 063840 (2013).
12. O. Sydoruk, V. Kalinin, and E. Shamonina, "Parametric amplification of magnetoinductive waves supported by metamaterial arrays," *Phys. Status Solidi* **244**(4), 1176–1180 (2007).
13. A. Rose and D. R. Smith, "Broadly tunable quasi-phase-matching in nonlinear metamaterials," *Phys. Rev. A* **84**(1), 013823 (2011).
14. A. Rose, D. Huang, and D. R. Smith, "Controlling the second harmonic in a phase-matched negative-index metamaterial," *Phys. Rev. Lett.* **107**(6), 063902 (2011).
15. C. Duncan, L. Perret, S. Palomba, M. Lapine, B. T. Kuhlmeiy, and C. M. de Sterke, "New avenues for phase matching in nonlinear hyperbolic metamaterials," *Sci. Rep.* **5**, 8983 (2015).
16. M. G. Silveirinha, "Nonlocal homogenization model for a periodic array of  $\epsilon$ -negative rods," *Phys. Rev. E Stat. Nonlin. Soft Matter Phys.* **73**(4), 046612 (2006).
17. M. G. Silveirinha, "Effective medium response of metallic arrays with Kerr-type dielectric host," *Phys. Rev. E* **87**, 165127 (2013).

18. S. M. Wang, S. Y. Mu, C. Zhu, Y. X. Gong, P. Xu, H. Liu, T. Li, S. N. Zhu, and X. Zhang, "Hong-Ou-Mandel interference mediated by the magnetic plasmon waves in a three-dimensional optical metamaterial," *Opt. Express* **20**(5), 5213–5218 (2012).
19. K. O'Brien, H. Suchowski, J. Rho, A. Salandrino, B. Kante, X. Yin, and X. Zhang, "Predicting nonlinear properties of metamaterials from the linear response," *Nat. Mater.* **14**(4), 379–383 (2015).
20. C. Cortes, W. Newman, S. Molesky, and Z. Jacob, "Quantum nanophotonics using hyperbolic metamaterials," *J. Opt.* **14**(6), 063001 (2012).
21. J. G. Hayashi, S. Fleming, B. T. Kuhlmeier, and A. Argyros, "Metal selection for wire array metamaterials for infrared frequencies," *Opt. Express* **23**(23), 29867–29881 (2015).
22. E. D. Palik, *Handbook of Optical Constants of Solids* (Academic Press, 1998).
23. K. W. DeLong, R. Trebino, J. Hunter, and W. E. White, "Frequency-resolved optical gating with the use of second-harmonic generation," *J. Opt. Soc. Am. B* **11**(11), 2206–2215 (1994).
24. B. Corcoran, C. Monat, M. Pelusi, C. Grillet, T. P. White, L. O'Faolain, T. F. Krauss, B. J. Eggleton, and D. J. Moss, "Optical signal processing on a silicon chip at 640Gb/s using slow-light," *Opt. Express* **18**(8), 7770–7781 (2010).

## 1. Introduction

Frequency conversion by nonlinear optical interaction is an effective means of generating electromagnetic radiation in spectral regions differing from the incident field [1,2]. Second-harmonic generation (SHG), for instance, can be used to convert incident radiation at a fundamental frequency (FF)  $\omega$  into radiation at the second-harmonic (SH) frequency  $2\omega$  [1]. In general, the phase of the SH wave component does not have the same spatial dependence as that of the FF wave. As a consequence, SH waves generated at different positions are not in phase and interfere destructively, strongly reducing the SHG efficiency [1]. Therefore, satisfying a phase-matching condition is of great importance to SHG processes, and is necessary for the SH waves to add in phase. For SHG, the phase-matching condition imposes the wave vector relation  $k_{2\omega} - 2k_{\omega} = 0$  [1,2], where  $k_{\omega,2\omega}$  are the wave numbers of the FF and SH, respectively. This condition is equivalent to the refractive index relation  $n(2\omega) = n(\omega)$ . However, phase matching is challenging to achieve because of material dispersion.

A common technique for achieving phase matching is *birefringent phase matching* [2]. By appropriately choosing the propagation direction in an anisotropic medium, the birefringence of the ordinary and the extraordinary wave cancels the phase mismatch due to dispersion. However, this is not possible for optically isotropic materials, and thus cubic materials such as GaAs, which otherwise have attractive nonlinear optical properties, have been little exploited for frequency conversion applications [3]. Another important technique is *quasi-phase matching* (QPM) [1,2], where efficient conversion can be achieved by periodically varying the sign of the nonlinearity by poling. However, this modulation of material properties is difficult to achieve, limiting the practical utility of this approach [4].

Periodicity in the linear properties of materials, for example in photonic crystals can also provide phase matching, by engineering the photonic bands of the structure [5–7]. Such structures can further enhance nonlinear conversion due to resonant and slow light effects [8]. However, to compensate for material dispersion photonic crystals need to be designed carefully. Phase matching is usually achieved near band edges, so that each photonic crystal design can only achieve phase matching over a limited bandwidth. For 1D photonic crystals, the magnitude of the refractive index modulation also limits the amount of material dispersion that can be compensated for [5].

Metamaterials, artificially engineered materials with sub-wavelength features, offer wide freedom to choose the structural arrangement of the constituents to yield exotic and desirable properties, such as negative refractive index [9], that are not available in natural materials. Metamaterials provide wide opportunities to achieve phase matching either by modifying dispersion relations [10–12], or by providing built-in quasi-phase matching [13,14]. Hyperbolic metamaterials, or indefinite media, a particular type of metamaterial, behave as a dielectric in one direction but like a metal in another [9]. As a consequence, their isofrequency surfaces, representing all allowed  $\mathbf{k}$ -vectors for a given frequency, are hyperbolic rather than

elliptical as in natural birefringent materials. This property allows the propagation of arbitrarily large wavenumbers, which, in principle, offers the possibility to compensate dispersion of any magnitude. Indeed, some of us previously showed that multi-layered hyperbolic metamaterials provide a number of means to achieve phase matching thanks to their unusual dispersion [15]. In this paper, we explore the possibility of achieving phase matching in hyperbolic wire metamaterials, subwavelength structures consisting of a dilute array of metal wires in a dielectric background. These behave like a metal in the direction parallel to the wires and like a dielectric orthogonal to them. While wire media and layered hyperbolic media are both hyperbolic, their effective properties differ significantly: which permittivity components are positive or negative, and their temporal and spatial dispersion differ such that the conditions to realize phase matching for wire media and for layered media [15] are very different, as we show here. While wire media are often periodic in two dimensions, and can thus be seen as a special case of photonic crystals, they differ from the latter in that the period of wire media is much smaller than the wavelength. The unusual properties of these media do not emerge from Bragg resonances – in fact, periodicity is not strictly required and random arrays of wires with sub-wavelength separation still behave as hyperbolic media. As a consequence, phase matching can be achieved over wide frequency bands in the same structure. However, this comes at the cost of additional losses due to the metallic inclusions.

Phase matching is a necessary but of course not sufficient condition to efficient second harmonic generation. Our aim here is to derive general rules on how far wire media can help achieving this necessary condition, rather than to look at specific designs and assessing their viability. To this effect, we require a linear calculation of modes of wire media, and can use existing analytic expressions of the homogenized dispersion relation to start our investigations [16]. Assessing the full conversion efficiency then also requires the calculation of the effective nonlinear properties, for example as discussed, or using microscopic modelling specific to particular implementations [17–20], beyond the scope of this study. We limit our study to the infrared part of the spectrum, where the real part of the permittivity of metals is large and negative and the losses are not too large [21]: in this regime, the permittivity orthogonal to wires is positive and non-resonant, which also restricts the number of cases to be considered. We apply a quadratic approximation to the nonlocal homogenization model [16] to analyze the frequency- and geometrical structure-dependent shape of the isofrequency contours of the modes in wire media. We then select all possible combinations of modes at the FF and SH and discuss the existence of phase matching solutions in each case. Finally, as an illustrative example, we consider gold wires embedded in GaAs for the mid-infrared frequency region. We verify the result with a full numerical simulation using a commercial finite element solver, showing that phase matching can be achieved without the uncertainties associated with the use of the effective medium approximation. This result proves that phase matching in wire metamaterials improves nonlinear conversion considerably, even when including propagation losses.

## 2. Normal surfaces of wire media

A schematic of the geometry of wire media is shown in Fig. 1(a). A periodic array of metal wires, each of radius  $r$  and permittivity  $\epsilon_m$ , is arranged in a dielectric host of permittivity  $\epsilon_h$ . The wires are arranged in a square lattice with period  $a$ . The medium is described in a Cartesian coordinate system in which the rods are oriented along  $z$ . In the long wavelength limit, *i.e.*,  $\lambda \gg a$ , wire media behave approximately like a spatially dispersive uniaxial material [16] with effective permittivity tensor  $\bar{\bar{\epsilon}} = \epsilon_h (\epsilon_{xx} \mathbf{xx} + \epsilon_{yy} \mathbf{yy} + \epsilon_{zz} \mathbf{zz})$ , and components

$$\epsilon_{xx} = \epsilon_{yy} = 1 + 2 \left[ \frac{\epsilon_m + \epsilon_h}{(\epsilon_m - \epsilon_h) f_V} - 1 \right]^{-1}, \quad (1)$$

$$\epsilon_{zz} = 1 + \left[ \frac{\epsilon_h}{(\epsilon_m - \epsilon_h) f_V} - \frac{\beta^2 - k_z^2}{\beta_p^2} \right]^{-1}, \quad (2)$$

where  $f_V = \pi r^2/a^2$  is the volume fraction of the wires,  $\beta = \sqrt{\epsilon_h} \omega/c$  is the wave number in the host medium, and  $\beta_p$  is the plasma wave number for perfectly conducting wires

$$(\beta_p a)^2 \approx \frac{2\pi}{\ln\left(\frac{a}{2\pi r}\right) + 0.5275}. \quad (3)$$

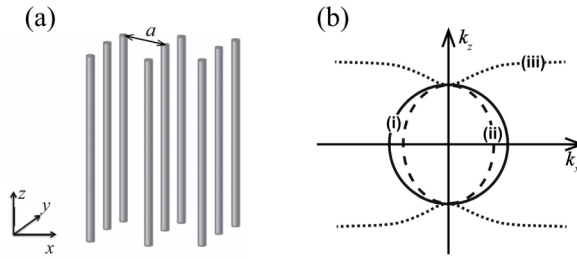


Fig. 1. (a) Schematic of wire media; (b) isofrequency surfaces of (i) TE (ordinary) mode (ii) First extraordinary (TM) mode (iii) Second extraordinary mode (quasi-TEM).

The homogenized properties lead to a dispersion relation for ordinary (TE) waves of the form  $k_x^2 + k_z^2 = \beta^2 \epsilon_{xx}$ . Uniquely, because of spatial dispersion, there are two extraordinary modes (rather than a single one), a TM mode and a quasi-TEM mode (see Fig. 1(b)). The propagation constants  $k_z^{(1)}$  and  $k_z^{(2)}$  of these modes satisfy the characteristic equation [16]

$$\begin{aligned} (k_z^{(1,2)})^2 = & \frac{1}{2} \left\{ \epsilon_{xx} (\beta^2 - k_x^2) + (\beta^2 + \beta_c^2 - \beta_p^2) \dots \right. \\ & \left. \pm \sqrt{[\epsilon_{xx} (\beta^2 - k_x^2) - (\beta^2 + \beta_c^2 - \beta_p^2)]^2 + 4\epsilon_{xx} \beta_p^2 k_x^2} \right\}, \end{aligned} \quad (4)$$

where  $\beta_c^2 = -[\epsilon_h/(\epsilon_m - \epsilon_h) f_V] \beta_p^2$  depends on geometry, materials and thus frequency.

The dispersion relations of the extraordinary modes given by Eq. (4) are implicit equations of  $k_x$ . It is therefore difficult to use them to derive general results on the existence or not of phase matching solutions. To this end, a Taylor expansion of Eq. (4) to 2nd order around  $k_x \approx 0$  is sufficient. This corresponds to paraxial incidence, but the results derived are bounds and our conclusions thus cover any incidence. The approximated expression takes the simplified form  $k_z^2 + c_x^{(1,2)} k_x^2 = c_0^{(1,2)}$ , where

$$c_0^{(1,2)} = \frac{1}{2} \left\{ (\epsilon_{xx} + 1) \beta^2 + (\beta_c^2 - \beta_p^2) \pm [(\epsilon_{xx} - 1) \beta^2 - (\beta_c^2 - \beta_p^2)] \right\}, \quad (5)$$

$$c_x^{(1,2)} = \frac{1}{2} \varepsilon_{xx} \left\{ 1 \pm \frac{(\varepsilon_{xx} - 1)\beta^2 - (\beta_c^2 + \beta_p^2)}{[(\varepsilon_{xx} - 1)\beta^2 - (\beta_c^2 - \beta_p^2)]} \right\}. \quad (6)$$

The signs of  $c_0$  and  $c_x$  determine the shape of the isofrequency surface when  $k_x \approx 0$ . Using the nomenclature of Duncan *et al* [15], a normal surface is north–south hyperbolic (NS) if  $c_0 > 0$ ,  $c_x < 0$ ; east–west hyperbolic (EW) if  $c_0 < 0$ ,  $c_x < 0$ ; elliptical if  $c_0 > 0$ ,  $c_x > 0$ ; evanescent if  $c_0 < 0$ ,  $c_x > 0$ .

We assume that both  $\varepsilon_m$  and  $\varepsilon_h$  are normally dispersive. Considerable insight can be gained from considering limiting cases in the approximation of good conductors, for which  $\varepsilon_{xx} \approx 1$ . Equations (5) and (6) have two limiting cases. (i) At low frequencies, *i.e.*,  $\beta_c^2 \ll \beta_p^2$ , the quasi-TEM mode is NS hyperbolic at  $k_x \approx 0$  and the TM mode tends to be evanescent. (ii) At high frequencies, *i.e.*,  $\beta_c^2 \gg \beta_p^2$ , the TM mode is elliptical with a similar dispersion relation to the TE mode, and a mode bound to the surfaces of the wires results from the coupling of surface plasmon polaritons (SPP) of the wires [16].

Figure 2(a) is a phase diagram showing the solutions as a function of frequency and filling fraction for gold wires in GaAs. The material permittivities of each material are taken from Palik [22]. The nominal boundary separating the two limiting cases is considered to be

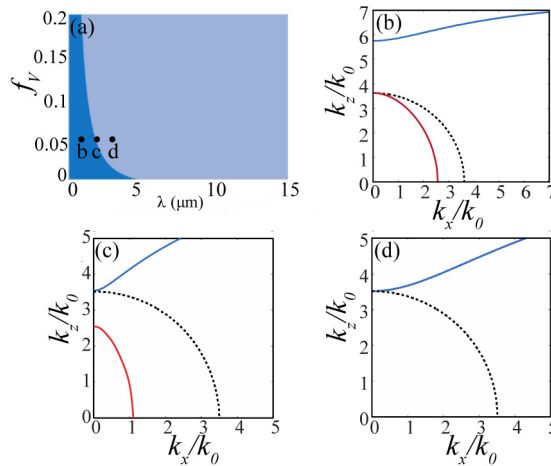


Fig. 2. (a) Phase diagram for a GaAs and gold wire medium from Eq. (4), showing the low-frequency (light blue) and high-frequency (dark blue) regimes versus wavelength and filling fraction  $f_v$ , for a structure with  $a = 150 \text{ nm}$ ,  $r = 20 \text{ nm}$ , *i.e.*,  $f_v = 5.6\%$ . (b)–(d) Dispersion relations of modes corresponding to the points indicated in (a), which refer to the three different frequency regimes. (b)  $\lambda = 1.55 \mu\text{m}$  (high frequency); (c)  $\lambda = 2.3 \mu\text{m}$  (intermediate frequency); (d)  $\lambda = 3.1 \mu\text{m}$  (low frequency). Dotted black curve: TE mode, red curve: TM mode, blue curve: second TM mode which is SPP like in (b) and quasi-TEM like in (c), (d).

$\beta_c^2 = \beta_p^2$ . While well away from this boundary, *i.e.*, in the limiting cases, the behavior is clear, the precise position of the boundary requires detailed calculations. Figures 2(b)–2(d) illustrate how the nature of the modes evolves with frequency for a given structure. Figure 2(b) shows the isofrequency curves in the high frequency regime (ii). In this regime there is an SPP-like mode and an elliptical TM mode which is tangent to the TE mode at  $k_x = 0$ . Figures 2(c) and 2(d) show the progression when shifting to lower frequencies: the elliptical

TM mode becomes evanescent and the quasi-TEM mode emerges; the latter is tangent to the TE mode at  $k_x = 0$ .

### 3. Phase matching in wire media

Considering the FF to be in the low frequency regime where the TM mode is evanescent, the results from Section 2 limit the possibilities for hyperbolic phase matching to the four cases shown in Table 1 and Fig. 3. We show below that a solution to the phase matching condition is guaranteed to exist for cases (A) and (C), for any combination of normally dispersive dielectric and metal. For case (D) phase matching does not occur, while for case (B) phase matching is not guaranteed, and, according to our simulations does not seem to occur.

**Table 1. The four possible combinations of modes for FF and SH for SHG in wire media, assuming the FF is in the low-frequency regime.**

Case	FF		SH	
	Mode	Shape	Mode	Shape
(A)	Quasi-TEM	NS	TE	Circular
(B)	Quasi-TEM	NS	Quasi-TEM	NS
(C)	Quasi-TEM	NS	TM	Elliptical
(D)	TE	Circular	Quasi-TEM	NS

*Case (A), (C) and (D):* In these cases, we seek general conditions under which a NS hyperbolic normal surface intersects with an ellipse or a circle. These are guaranteed to intersect if the vertical intercept of the hyperbola is smaller than that of the circle or ellipse (Figs. 3(a) and 3(c)). Case (D) can be eliminated because for a normal dispersive dielectric the minimum phase index at the SH exceeds the maximum at the FF (Fig. 3(d)). From Eq. (4), for case (A) and (C), the necessary and sufficient condition for phase matching is

$$\varepsilon_{xx}(2\omega)\varepsilon_h(2\omega) > \varepsilon_{xx}(\omega)\varepsilon_h(\omega). \quad (7)$$

This is always satisfied if the host material is normally dispersive. An ordinary-extraordinary phase matching solution is thus guaranteed to exist (Case (A)); an extraordinary-extraordinary phase matching exists if the SH TM mode is not evanescent (case (C)). This conclusion is drawn independently of the structure and fundamental frequency – thus within our approximations (namely that frequencies are in the infrared or lower, and the periodicity is much smaller than the wavelength) any geometry of wire array provides SHG phase matching for any FF/SH frequency pair – this is in stark contrast to phase matching provided by photonic crystals which need to be designed for a specific frequency pair.

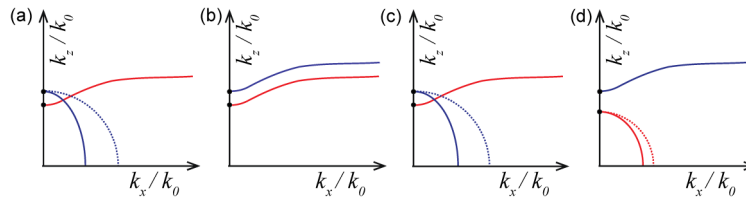


Fig. 3. Typical isofrequency contours for the four cases of FF (in red) and SH (in blue) from Table 1. Extraordinary and ordinary waves are indicated by solid and dashed curves, respectively. Phase matching solution is guaranteed to exist in cases (A) and (C). In case (B) a phase matching solution is not guaranteed. Phase matching is impossible in case (D).

*Case (B):* The minimum of the isofrequency curves quasi-TEM modes is lower for the FF than for the SH (see Fig. 3(b)), and the curves flatten at high  $k_x$  values due to spatial dispersion. The two normal surfaces can only intersect before they flatten out at large  $k_x$ . Such a crossing was not observed in our simulations for the wavelengths and materials of interest. Hence, phase matching is not guaranteed in this case.

#### 4. Simulation results and discussion

To confirm the results obtained using the effective medium approach, we performed detailed numerical calculations of the full structure using a commercial finite element method (FEM) solver (COMSOL). We considered an infinitely long wire array with a square periodic lattice, applying Bloch-Floquet boundary conditions at the edges of the numerical domain, and calculated the linear modes of the structure to obtain the isofrequency curves. Figure 4(a) and 4(b) shows results for gold wires in GaAs in the mid-infrared region (FF at  $\lambda = 3.1 \mu\text{m}$ ) of the spectrum, corresponding to Cases (A) and (C) in Table 1. The extraordinary-extraordinary matching solution (circled in Fig. 4(a)) is obtained at  $k_x/k_0 \approx 0.45$ ,  $k_z/k_0 \approx 3.45$  between the FF TEM and SH TM. An extraordinary-ordinary matching solution (circled in Fig. 4(b)) is obtained at  $k_x/k_0 \approx 0.62$ ,  $k_z/k_0 \approx 3.56$  between the FF TEM and SH TE. The FEM simulations also provide propagation losses, and thus propagation lengths in the selected wire media for all modes. For FF and SH these are  $45 \mu\text{m}$  and  $23.5 \mu\text{m}$  respectively, which is substantially larger than the coherence length for GaAs which is  $L = 12.5 \mu\text{m}$  at FF  $3.1 \mu\text{m}$  [2]. The FF pump thus propagates with reasonable losses over four coherence lengths, and since the phase matched SHG signal grows quadratically with distance we may expect a 16 time enhancement in the lossy wire medium compared to the isotropic medium. Indeed, solving for SHG intensity using the slowly varying envelope approximation [1,2], taking into account absorption losses of both the FF and SH, and assuming the same nonlinear coefficient as the host medium, gives a maximum SHG after  $46 \mu\text{m}$  of propagation in the wire medium, with an 18x enhancement in SHG intensity compared with the maximum obtained in non-phase matched GaAs. Given the short propagation lengths, walk-off is also unlikely to be an issue for any pulses longer than 100 fs. Thus using a wire array in this case could result in considerably higher SH generation efficiency than from unstructured GaAs. This comparison confirms that this method of phase matching, while limited by losses, remains realistic for small structures. Of course, because of the large losses, wire arrays cannot be expected to compete with phase-matched SHG in naturally anisotropic dielectric crystals which are virtually lossless. Wire arrays are also unlikely to beat quasi-phase matched SHG in dielectrics or phase matched SHG in carefully designed photonic crystals. However, wire arrays can provide phase matching for materials that are not naturally anisotropic, and contrary to quasi phase matching and photonic crystals, the same wire structure can provide phase matching over a virtually unlimited frequency range, which may find use for applications such as ultrashort pulse characterization techniques [23] or optical signal quality monitoring [24].

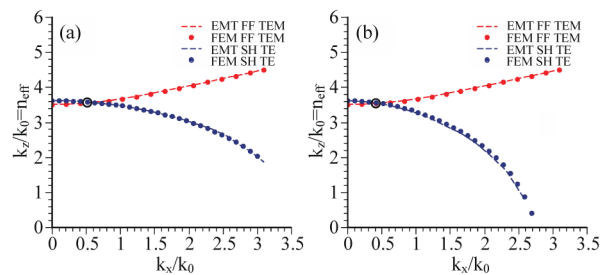


Fig. 4. Isofrequency contours calculated by FEM (dots) compared with an effective medium approach (dashed curves) for gold wires in GaAs with  $a = 150 \text{ nm}$ ,  $r = 20 \text{ nm}$ , with FF  $\lambda = 3.1 \mu\text{m}$ . Phase matching solutions for (a) FF TEM and SH TE (b) FF TEM and SH TM are circled.

#### 5. Conclusion

A systematic analysis of the possibility of SHG phase matching using the hyperbolic dispersion of wire media metamaterials shows that phase matching can always be achieved in

the mid-infrared part of the spectrum (3  $\mu\text{m}$  to 10  $\mu\text{m}$ ). We confirm this finding by full numerical calculation. We surmise that phase matching of other nonlinear frequency conversion processes can be similarly achieved by exploiting the dispersion of wire media.

### **Acknowledgments**

The authors thank Drs Mikhail Lapine and Stefano Palomba for discussions during the early stages of this work. This work was supported by the Australian Research Council (CUDOS Centre of Excellence CE110001018).